Network Topology Optimization for Optical Networks in Aircraft Using MILP

Bjoern Annighoefer
Institute of Aircraft Systems
University of Stuttgart
Stuttgart, Germany
0000-0002-1268-0862

Adrian Zeyher
Institute of Aircraft Systems
University of Stuttgart
Stuttgart, Germany
0000-0003-2888-4509

Johannes Reinhart
Institute of Aircraft Systems
University of Stuttgart
Stuttgart, Germany
0000-0002-3512-5220

***Abstract*—Distributed Integrated Modular Avionics (DIMA) are state of the art in modern aircraft systems. It is a safety-critical, shared computing system with a common network. The architectural complexity of DIMA grows steadily since also the number of functions increases. An optimal DIMA system is hardly retrieved by manually, but finding the optimum can be supported with automated design procedures. In particular, the topology optimization of networks underlying the DIMA architecture is resource intensive and time consuming. For optical networks, which are planned for future systems, the known topology optimization algorithms are only partially appropriate. We propose an algorithm for automated topology optimization of optical networks based on Mixed-integer Linear Programming (MILP). The algorithm derives a global optimum from a given solution space in terms of the interconnection of devices, routing of signals, the placement of opaque or translucent switches, the fiber core count per cable, and ensures a valid attenuation level at each cable and connector. The algorithm is demonstrated with optimizing an in-flight entertainment system's optical network topology with 23 devices and 48 signals.**

***Index Terms*—attenuation, damping, connectors, optical power, opaque switch, IMA, MILP, avionics, multi-core fiber**

I. Introduction

Modern large transport airplanes are based on Distributed Integrated Modular Avionics (DIMA). DIMA is a concept for sharing computing and network resources in a safety-critical manner. Generic computer modules are installed throughout the aircraft fuselage. Locally, I/O modules read sensors and control actuators. Centrally placed processing modules calculate control commands. All DIMA modules are connected with a high-bandwidth Aircraft Data and Communication Network (ADCN). The modules and network are configurable. The planning and development of a DIMA avionics system architecture is time and resource intensive, due to a high number of software components, signals, modules, peripherals as well as a complex interaction. It is assumed that potential is wasted and a (partial) automation of design steps results in better reliability, weight, and cost of the system [1, p. 2]. Special attention is paid to the network connecting the modules. Many implemented functions are safety-relevant and have mandatory reliability and latency requirements. A prominent example is the flight control system. Since the number of functions increases exponentially with time [2], the ADCNs used today will reach their limits in terms of data rate and latency in a foreseeable time. Optical networks are being considered for future deployments as an alternative to the commonly used ARINC 629 and ARINC 664 (AFDX) networks [3]. This work presents a Mixed-Integer Linear Programming (MILP) model, which generates an optimal network topology for a given installation space from a given set of signals and optical components. The algorithm considers necessary signal flows, cable properties such as attenuation and the number of fibers, and generic resource constraints of hardware and locations. The remainder of this work is organized as follows. Chapter II defines our topology optimization problem. In Chapter III we review the state-of-the-art and compare it to our approach. Chapter IV derives the MILP model. In chapter V the algorithm is applied to optimize the network of an In-flight Entertainment System (IFE). Chapter VI discusses the results and gives an outlook.

This paper is based on research work carried out in the DELIA project (contract code: 16KIS0940) funded by the German Federal Ministry of Education and Research (BMBF) in the IKT 2020 program.

II. Topology Optimization Problem Definition

The general scope of topology optimization in this work is depicted in fig. 1. We assume a given installation space for the optical network consisting of possible installation spaces for switches and end systems as well as cable routes. Within this installation space a number of end systems exists that have communications needs in terms of signals that have to be transmitted and received. Given the installation locations and possible cable routes, an optimal optical network is searched that connects all end systems and fulfills their communication needs. The communication needs are fulfilled if a path from sender to receiver for each signal is determined. In addition, minimum weight, cost, and installation effort are of interest. The optical network has to be built from predefined switch and cable types. Switches can either be opaque or translucent. Opaque switches convert optical information to electrical and back and, therefore, decouple the optical power of connected cables. Translucent switches forward the original optical signal, i.e. input and output power levels are dependent. Moreover, switches can differ in the number of ports and costs as well as in the resources required for their installation (e.g. space) and internal resources required for the signal routing

978-3-903176-33-1

(e.g. bandwidth or number of signals). Cables differ in cost and weight. Multi-core fiber cables are assumed, and different cable types can have different numbers of cores. It is defined that each signal requires a single core, because current ADCNs enforce a strict signal segregation for safety reasons, and multi-core fibers exhibit an almost perfect physical segregation. A valid topology has to stay within the resources of the installation spaces and cable routes. A valid routing has to stay within the resources of the switches and the optical power level of signals has to be in the range acceptable for the individual components. Attenuation is to be considered in cables, connectors, and translucent devices. Multiple optimization objectives exist, e.g. the cost or weight of the network components, the installation effort, and the number of components in total. An a priori definition of fixed switches or cables shall be possible.

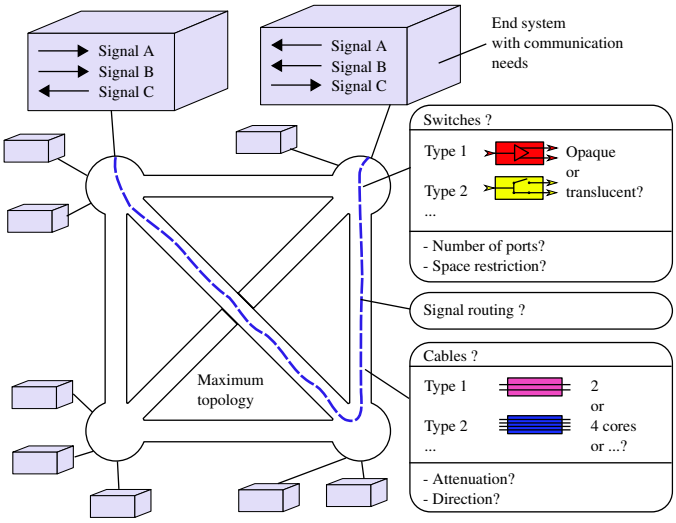

Fig. 1. Scope of the topology optimization

III. Related Work

Optimization is a common issue for (optical) networks. Typical subjects of optimization are routing [4]–[11], scheduling [6], [7], [12], robustification [11], [13], and frequency sharing [9], [14]. The mentioned works are exemplary and the list is not complete. Some of the works address multiple issues at once. MILP or ILP are common methods to solve the problems. Whereas the existing solutions for routing match our needs, the underlying network topology needs to be predefined. That is not the case for our problem. Topology optimization is a less frequent research topic, but is has been addressed for electrical [15]–[18] and optical networks [19]–[25]. The approaches for electrical networks miss optical properties as attenuation and multi-core cables. The approaches for optical networks are very domain-specific, and deal with special applications (e.g. telecommunication, dynamic routing) or certain optical network technologies (e.g. WDM) that do not match our setup. In no existing approach the placement and choice of components is subject to optimization. The approach most similar to our needs is [26]. It suggests a Binary Program representation for a topology optimization of Ethernet-like networks. The approach considers switch types, port, and resource restrictions as well as signal routing and signal segregation constraints. We extend that approach to optical networks by adding multi-core cable types and attenuation.

IV. Topology Optimization as a MILP

The topology optimization is modeled as a MILP problem, i.e. $\max f^{\mathsf{T}} x$ subject to $Ax \leq b$. The encoding of the expected topology in the solution vector is:

$$x = (x^{D_k}_{\mathcal{T}_l}, \ldots \in \{0, 1\} \quad (1)$$

$$, x^{F_j}_{\mathcal{T}_t}, \ldots \in \{0, 1\} \quad (2)$$

$$, x^{F_j}_{\text{useAB}}, x^{F_j}_{\text{useBA}} \in \mathbb{Z} \quad (3)$$

$$, x^{F_j}_{\text{allowAB}}, x^{F_j}_{\text{allowBA}}, \ldots \in \{0, 1\} \quad (4)$$

$$, x^{S_i}_{F_j,\text{AB}}, x^{S_i}_{F_j,\text{BA}}, \ldots \in \{0, 1\} \quad (5)$$

$$, x^{S_i}_{D_k,\text{doesRx}}, x^{S_i}_{D_k,\text{doesTx}}, x^{S_i}_{D_k,\text{Rx}}, x^{S_i}_{D_k,\text{transm.}} \in \{0, 1\} \quad (6)$$

$$, x^{S_i}_{D_k,\text{TxAvail}}, x^{S_i}_{D_k,\text{Tx}}, x^{S_i}_{F_j,\text{powerAB}}, x^{S_i}_{F_j,\text{powerAB}} \in \mathbb{R} \quad (7)$$

$$, x^{S_i}_{D_k,\text{opaqueRx}} \in \{0, 1\}). \quad (8)$$

x is based on the fact that the maximum topology is calculated a priori from the given installation space, i.e. the maximum number of switch devices and links is known. Variables (1) and (2) encode the existence of all possible devices and cables of their chosen type. The set $\mathcal{D}$ denotes all possible devices in the network. The element $D_k \in \mathcal{D}$ is the kth device. The total number of devices is denoted by $|\mathcal{D}|$. $\mathcal{F}$ represents the set of all potential cables. A fully connected graph is assumed. A single cable of this set is referred to as $F_j \in \mathcal{F}$. $|\mathcal{F}|$ is the total number of possible cables. The notation $F_j = (D_A, D_B)$ expresses which two devices D_A and D_B are connected by cable F_j, with $D_A \neq D_B$. Two cables F_m and F_n linking the same pair of devices D_A and D_B are legal. Furthermore, the direction is considered, i.e. $(D_A, D_B) \neq (D_B, D_A)$. $\mathcal{T}$ is the set of all types, whereas types are divided into device (switch) l and cable types t. Variables (3) and (4) encode the used fiber cores count and the transmission direction per cable. Signals are represented by the set $\mathcal{S}$, the signal count is $|\mathcal{S}|$. Source and target D_S and D_T of a signal $S_i \in \mathcal{S}$ are indicated by the notation $S_i = (D_S, D_T)$. Multiple signals are allowed between the same source and target device, but signal aggregation is recommended as each signal requires its own core. Bandwidth limitations have to be considered in signal aggregation. Variables (5) and (6) encode the path for each signal on each device and cable, i.e. the routing. The encoding of device, cable, and type usage as well as encoding and constraints for signals routes and resource constraints are skipped here because they equal the ones proposed in [26]. The complete description of the topology optimization MILP can be found in the extended version of this paper [27]. In the following, we focus on the MILP representation of optical power limits, i.e. variables (7) and (8).

A. Attenuation

An upper and lower bound for the signal strength in the network is required to formulate the attenuation or power constraints. A fully connected network with $|\mathcal{D}|$ devices is assumed. The longest possible signal path in it passes all $|\mathcal{D}|$ devices. Only translucent intermediate devices are of interest for the power considerations. Opaque devices can re-power the signal. Between each pair of devices, the signal is transmitted via a cable. In total, this results in $|\mathcal{D}| - 1$ cables in the signal path assuming that each device is not passed more than once. The signal power at the receiving device is calculated by adding the transmit power to all attenuations occurring along the signal path. Conversely, the transmit power can be calculated starting from the receive power. Inserting maximum and minimum attenuation values yields the extreme conditions. A positive attenuation value is signal amplification. Maximum attenuation correlates with the smallest attenuation value. The minimum attenuation or gain correlates with the largest attenuation value. With (9) a general limit is derived. All power values occurring in the network have to be within in the interval $[-P_{lim}, P_{lim}]$.

$$\begin{aligned} P_{lim} = {} & P_{lim,Tx} + \left(|\mathcal{D}| - 2\right) \cdot P_{lim,\Delta_\mathcal{D}} \\ & + \left(|\mathcal{D}| - 1\right) \cdot P_{lim,\Delta_\mathcal{F}} + P_{lim,Rx} \geq 0 \end{aligned} \tag{9}$$

The four terms necessary are calculated from the maximum and minimum values of the cable and device types. First, $P_{lim,Tx}$ denotes the largest absolute transmit power. For the optimization only the largest maximum as well as the smallest minimum transmit power $\hat{\tau}^{\mathcal{D}}_{\overline{\text{Tx}}}$ and $\check{\tau}^{\mathcal{D}}_{\underline{\text{Tx}}}$ are required. Since $\check{\tau}^{\mathcal{D}}_{\underline{\text{Tx}}} \leq \check{\tau}^{\mathcal{D}}_{\overline{\text{Tx}}} \leq \hat{\tau}^{\mathcal{D}}_{\overline{\text{Tx}}}$ and $\check{\tau}^{\mathcal{D}}_{\underline{\text{Tx}}} \leq \hat{\tau}^{\mathcal{D}}_{\underline{\text{Tx}}} \leq \hat{\tau}^{\mathcal{D}}_{\overline{\text{Tx}}}$, $\hat{\tau}^{\mathcal{D}}_{\underline{\text{Tx}}}$ and $\check{\tau}^{\mathcal{D}}_{\overline{\text{Tx}}}$ are eliminated, i.e. the largest minimum and smallest maximum transmit power are removed:

$$P_{lim,Tx} := \max\left(\left|\check{\tau}^{\mathcal{D}}_{\underline{\text{Tx}}}\right|, \left|\hat{\tau}^{\mathcal{D}}_{\overline{\text{Tx}}}\right|\right) \tag{10}$$

In the same way, $P_{lim,Rx}$ represents the largest received power. Again, the calculation requires only the largest maximum and smallest minimum power $\hat{\tau}^{\mathcal{D}}_{\overline{\text{Rx}}}$ and $\check{\tau}^{\mathcal{D}}_{\underline{\text{Rx}}}$. Similar to the receive power $\check{\tau}^{\mathcal{D}}_{\underline{\text{Rx}}} \leq \check{\tau}^{\mathcal{D}}_{\overline{\text{Rx}}} \leq \hat{\tau}^{\mathcal{D}}_{\overline{\text{Rx}}}$ and $\check{\tau}^{\mathcal{D}}_{\underline{\text{Rx}}} \leq \hat{\tau}^{\mathcal{D}}_{\underline{\text{Rx}}} \leq \hat{\tau}^{\mathcal{D}}_{\overline{\text{Rx}}}$, the smallest maximum as well as largest minimum received power $\check{\tau}^{\mathcal{D}}_{\overline{\text{Rx}}}$ and $\hat{\tau}^{\mathcal{D}}_{\underline{\text{Rx}}}$ do not need to be considered.

$$P_{lim,Rx} := \max\left(\left|\check{\tau}^{\mathcal{D}}_{\underline{\text{Rx}}}\right|, \left|\hat{\tau}^{\mathcal{D}}_{\overline{\text{Rx}}}\right|\right) \tag{11}$$

The remaining two terms are determined similarly. $P_{lim,\Delta_\mathcal{D}}$ is determined by the largest absolute value of the internal device attenuation. The maximum absolute value of the cable-side transmission loss is used for the $P_{lim,\Delta_\mathcal{F}}$.

$$P_{lim,\Delta_\mathcal{D}} := \max\left(\left|\check{\tau}^{\mathcal{D}}_{\Delta}\right|, \left|\hat{\tau}^{\mathcal{D}}_{\Delta}\right|\right) \tag{12}$$

$$P_{lim,\Delta_\mathcal{F}} := \max\left(\left|\check{\tau}^{\mathcal{F}}_{\Delta}\right|, \left|\hat{\tau}^{\mathcal{F}}_{\Delta}\right|\right) \tag{13}$$

1) Cable attenuation: The power calculation is carried out according to an adapted calculation rule derived from [28] and [29]. Along the signal path, starting with the transmitted power, all attenuation influences are accumulated. The largest attenuations are scattering and absorption effects in cables and devices as well as mechanical inaccuracies in the alignment. The latter is referred to as an insertion loss at connectors. The insertion loss is not assigned to the devices, but is considered as a part of the cable design. All attenuations along a cable $F_j \in \mathcal{F}$ are assumed to be summable to a single attenuation value $p^{F_j}_{\Delta}$. This is possible since the length of each cable is known from the installation space dimensions. Furthermore, it is assumed that the plug-in or splice connections are included in this attenuation value. The basic idea of the power calculation is to add up the segment's individual attenuations. Therefore, the calculation is carried out in decibels, which leads to an additive expression compatible to MILP. However, since no signal path information is available when setting up the MILP constraints, all possible paths have to be considered. This leads to the model shown in fig. 2.

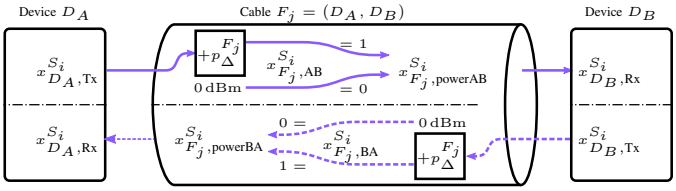

Fig. 2. Power flow along a cable $F_j = (D_A, D_B)$ for a signal S_i. The upper half of the figure shows how the power information propagates in the cable direction. The power flow against the direction is shown in the lower half of the figure.

For each signal $S_i \in \mathcal{S}$ and each cable $F_j \in \mathcal{F}$ a set of constraints is defined, which calculates the power change along cable F_j depending on the signal path. The path as well as the powers depend on the direction. If the signal S_i is transmitted as depicted in fig. 2 from device D_A to device D_B, then the signal power at the cable's end, $x^{S_i}_{F_j,\text{powerAB}}$, is obtained by adding the cable attenuation $p^{F_j}_{\Delta}$ to the transmit power $x^{S_i}_{D_A,\text{Tx}}$ of D_A to be determined. The attenuation value is negative if signal attenuation occurs. Therefore, the attenuation has to be added. If the signal is not transmitted over that link, then $x^{S_i}_{F_j,\text{powerAB}} = 0\,\text{dBm}$ is applied to the power at the cable's end. This choice is reasonable for the attenuation consideration in the devices. For the opposite direction $B \rightarrow A$ the conditions apply analogously. Formally, these conditions can be described mathematically as follows. $x^{S_i}_{F_j,\text{AB}}$ is the transmission state.

$$x^{S_i}_{F_j,\text{powerAB}} = \begin{cases} x^{S_i}_{D_A,\text{Tx}} + p^{F_j}_{\Delta} & \text{if } x^{S_i}_{F_j,\text{AB}} = 1 \\ 0 & \text{if } x^{S_i}_{F_j,\text{AB}} = 0 \end{cases} \tag{14}$$

$$x^{S_i}_{F_j,\text{powerBA}} = \begin{cases} x^{S_i}_{D_B,\text{Tx}} + p^{F_j}_{\Delta} & \text{if } x^{S_i}_{F_j,\text{BA}} = 1 \\ 0 & \text{if } x^{S_i}_{F_j,\text{BA}} = 0 \end{cases} \tag{15}$$

Eight inequalities are needed for a MILP compatible notation using the Big-M method [30, S. 2].

B. Attenuation Consideration in Devices

The challenge is to model opaque and translucent devices by a common set of constraints. Separation is not possible due to the common type model.

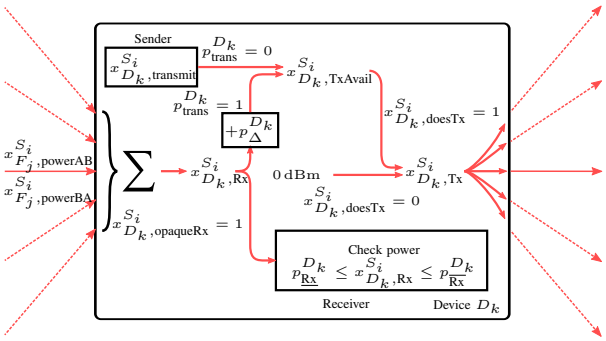

Fig. 3. Power flow within a device D_k for a signal S_i. The mixture of opaque and translucent devices creates complex attenuation considerations.

1) Received Power: Fig. 3 shows how power flows through a device $D_k \in \mathcal{D}$. Assuming that at most one cable F_j carries the signal $S_i \in \mathcal{S}$ to the device, the incoming signal strength is calculated by summation. For this purpose the power at the cable's end is set to $0\,\mathrm{dBm}$ when no signal is transmitted. This incoming signal power $x^{S_i}_{D_k,\text{Rx}}$ corresponds to the power at the end of the cable transmitting to the device:

$$x^{S_i}_{D_k,\text{Rx}} = \sum_{F_j \in \{\mathcal{F} | F_j = (*, D_k)\}} x^{S_i}_{F_j,\text{powerAB}} + \sum_{F_j \in \{\mathcal{F} | F_j = (D_k, *)\}} x^{S_i}_{F_j,\text{powerBA}} \tag{16}$$

The auxiliary variable $x^{S_i}_{D_k,\text{opaqueRx}}$ encodes whether an opaque type is assigned to the associated device D_k and the signal S_i is received by the device. It is determined from combination of the receive state $x^{S_i}_{D_k,\text{doesRx}}$ and the complementary value of the device property $p^{D_k}_{\text{trans}}$. According to the general encoding of logical conditions in [31, 4 ff] this results in the inequalities:

$$x^{S_i}_{D_k,\text{opaqueRx}} \le x^{S_i}_{D_k,\text{doesRx}} \tag{17}$$

$$x^{S_i}_{D_k,\text{opaqueRx}} \le \left(1 - p^{D_k}_{\text{trans}}\right) \tag{18}$$

$$x^{S_i}_{D_k,\text{opaqueRx}} \ge \left(1 - p^{D_k}_{\text{trans}}\right) + x^{S_i}_{D_k,\text{doesRx}} - 1 \tag{19}$$

If the device D_k is opaque, then the received power should neither overpower the sensor ($p^{D_k}_{\overline{\text{Rx}}}$) nor be below its sensitivity $p^{D_k}_{\underline{\text{Rx}}}$. Formally, however, it is considered whether the signal S_i is received at all. Indeed, if there is no reception, then in the received power $x^{S_i}_{D_k,\text{Rx}} = 0$ is meaningless and the sensitivity is not considered. All incoming signal powers are zero, thus their sum is also zero. A check is performed if the device D_k is opaque and the signal S_i is received. This condition is represented by the auxiliary variable $x^{S_i}_{D_k,\text{opaqueRx}}$. Formally, the implication below is obtained with the decision variable $x^{S_i}_{D_k,\text{opaqueRx}}$:

$$x^{S_i}_{D_k,\text{opaqueRx}} = 1 \quad \Longrightarrow \quad p^{D_k}_{\underline{\text{Rx}}} \le x^{S_i}_{D_k,\text{Rx}} \le p^{D_k}_{\overline{\text{Rx}}} \tag{20}$$

As before, this is modeled with a Big-M notation. Again, the power limit P_{lim} is used as the Big-M constant.

$$x^{S_i}_{D_k,\text{Rx}} - p^{D_k}_{\overline{\text{Rx}}} \le P_{lim} \cdot \left(1 - x^{S_i}_{D_k,\text{opaqueRx}}\right) \tag{21}$$

$$-x^{S_i}_{D_k,\text{Rx}} + p^{D_k}_{\underline{\text{Rx}}} \le P_{lim} \cdot \left(1 - x^{S_i}_{D_k,\text{opaqueRx}}\right) \tag{22}$$

It should be noted that attenuations occurring during reception in the device are not modeled. If an optical path to the sensor inside the opaque device degrades the signal, this attenuation is added to the sensitivity range in advance during the type declaration. Further possibly desired margins are to be added in advance to the declaration.

2) Signal Dispatch and Internal Attenuation: The power calculation of the signal dispatch requires several steps. First, the theoretically available transmit power $x^{S_i}_{D_k,\text{TxAvail}}$ is determined. In the case of opaque devices, this corresponds directly to the actual transmitter power $x^{S_i}_{D_k,\text{transmit}}$. For translucent devices, the available transmit power is calculated from the received power $x^{S_i}_{D_k,\text{Rx}}$ and the internal attenuation $p^{D_k}_{\Delta}$ of the device:

$$x^{S_i}_{D_k,\text{TxAvail}} = \begin{cases} x^{S_i}_{D_k,\text{Rx}} + p^{D_k}_{\Delta} & \text{if } p^{D_k}_{\text{trans}} = 1 \\ x^{S_i}_{D_k,\text{transmit}} & \text{if } p^{D_k}_{\text{trans}} = 0 \end{cases} \tag{23}$$

The decision variable $p^{D_k}_{\text{trans}} = 1$ encodes whether an opaque or translucent device is present. At this point, the device attenuation of translucent devices is included. For opaque devices there is no consideration of attenuation values. If present, those are considered with the transmitter power as part of the device type declaration. The inclusion of the case distinction (23) is based again on Big-M.

The transmitter power $x^{S_i}_{D_k,\text{transmit}}$ is freely selectable within a power range $\left[p^{D_k}_{\underline{\text{Tx}}},\ p^{D_k}_{\overline{\text{Tx}}}\right]$. Consequently, transmitters with adjustable power can be considered in the optimization. A distinction between opaque and translucent devices is not made. For the latter, the range is set to $\{0\}$. Moreover, an additional constraint is required:

$$p^{D_k}_{\underline{\text{Tx}}} \le x^{S_i}_{D_k,\text{transmit}} \le p^{D_k}_{\overline{\text{Tx}}} \tag{24}$$

The available transmit power $x^{S_i}_{D_k,\text{TxAvail}}$ is calculated independently of the fact whether the device D_k transmits the signal S_i at all. The latter is stored in the status variable $x^{S_i}_{D_k,\text{doesTx}}$. If S_i is not transmitted, a transmit power of $0\,\mathrm{dBm}$ is desired. A case differentiation is introduced for calculating the actual transmitted signal power $x^{S_i}_{D_k,\text{Tx}}$:

$$x^{S_i}_{D_k,\text{Tx}} = \begin{cases} x^{S_i}_{D_k,\text{TxAvail}} & \text{if } x^{S_i}_{D_k,\text{doesTx}} = 1 \\ 0 & \text{if } x^{S_i}_{D_k,\text{doesTx}} = 0 \end{cases} \tag{25}$$

When the signal S_i is transmitted, the actual transmit power $x^{S_i}_{D_k,\text{Tx}}$ is equal to the available power $x^{S_i}_{D_k,\text{TxAvail}}$. If no

transmission takes place, the transmit power is zero. The case discrimination (25) is again represented by four constraints using the Big-M method. The absolute power bound P_{lim} is used as a limit.

V. Optimizing an Optical IFE Network

An In-flight Entertainment system (IFE) scenario is used for demonstration. The optimization is implemented in Python. The scenario is modeled with the Open Avionics Architecture Model (OAAM) [32]. The MILP problem is solved using Gurobi 8.1.0 on a Intel Core i3-2100 with 8 GB RAM.

A. Scenario setup

The scenario comprises three rows of seats of an aircraft with a center aisle. Each row of seats consists of two groups of seats, one to the left and one to the right of the aisle. Each of these seating groups contains a central computer, called a *Seat Unit*, which controls the screens and controls. There is a panel above each seating group with call buttons, indicator, and reading lights. Each panel has a dedicated control unit, i.e. *Call and Light Panel*. The IFE is able to display live TV and movies at each seating area. Two streaming computers (*Stream Server*) provide the data to be transmitted over the optical network. Both *Stream Servers* can provide each seating group with a video stream. The *Stream Servers* also control the lamps of the *Call and Light Panels*. All inputs to the control elements of the seating groups and the call buttons are processed by two *Control Servers*. These command also the *Stream Servers*. In a real aircraft, multiple of these aisle segments would be placed sequentially. The optimization space for the IFE scenario and the optimal solution are shown in fig. 4. The points outlined in black represent potential positions for switches. There are two switch types to choose from, namely an opaque and a translucent one. All other devices have their type already assigned. Table I lists the available device types and their properties. With the exception of one translucent switch, all devices are opaque. No cost values are assigned to fixed device types. It is assumed that a translucent device is less expensive than an opaque device that requires active components. The available cable types are listed in table II. They all have the identical attenuation characteristics, but differ based on their number of cores. The chosen numbers are inspired by the [33] datasheet. The optimization objective is the total cost for cables and switches:

TABLE I
Device type properties in the IFE scenario. RX and TX are in dBm. Entries marked with — are modeled as zero.

Name	$\tau^{\mathcal{D}}_{\text{ports}_t}$	$\tau^{\mathcal{D}}_{\Delta_t}$	$\tau^{\mathcal{D}}_{\underline{\text{Rx}}_t}$	$\tau^{\mathcal{D}}_{\overline{\text{Rx}}_t}$	$\tau^{\mathcal{D}}_{\underline{\text{Tx}}_t}$	$\tau^{\mathcal{D}}_{\overline{\text{Tx}}_t}$	$\tau^{\mathcal{D}}_{\text{trans}_t}$	$\tau^{\mathcal{D}}_{\text{cost}_t}$
Call and Light Panel	2	—	-14	0.5	-5	0	0	—
Seat Unit	2	—	-14	0.5	-5	0	0	—
Switch Opaque	6	—	-14	0.5	-5	0	0	6000
Switch Translucent	6	-0,5 dB	—	—	—	—	1	5600
Stream Server	3	—	-14	0.5	-5	0	0	—
Control Server	3	—	-14	0.5	-5	0	0	—

$$\text{minimize} \quad \sum_{D_k \in \mathcal{D}} \tau^{D_k}_{cost} + \sum_{F_j \in \mathcal{F}} \tau^{F_j}_{cost} \tag{26}$$

TABLE II
Cable types in IFE scenario. All cable types are bidirectional. Attenuation includes connectors and internal cable losses.

Name	$\tau^{\mathcal{F}}_{\text{cores}_t}$	$\tau^{\mathcal{F}}_{\Delta_t}$	$\tau^{\mathcal{F}}_{\text{cost}_t}$
Optical Wire 2 Core	2	$-2\,\text{dB}$	10
Optical Wire 4 Core	4	$-2\,\text{dB}$	40
Optical Wire 8 Core	8	$-2\,\text{dB}$	80
Optical Wire 12 Core	12	$-2\,\text{dB}$	90

Only the connection between the two *Stream Servers* 20 and 21, as well as the connection between the two *Control Servers* 22 and 23 is limited to the two-core cable type. Other cable types are subject to the optimization. In total, there are 48 necessary signals for this scenario. The detailed list of signals is given in [27].

B. Optimization

The IFE scenario resulted in a MILP with 17 876 variables and 49 316 inequalities. It took 9 min to retrieve a global optimal solution. The entire program execution required 23 min, of which a total of 6 min are spent on data input, output, and internal model building. Another 6 min are attributable to Gurobi and subsequent processing. The optimized topology is shown fig. 4. Six of the eight possible switches are instantiated in the topology as translucent devices (yellow). No opaque switches are instantiated. Two possible switch positions are unused. The cable assignment is symmetrical along one axis. Although there is a symmetry of the defined signals in in the top strands (0-4 and 5-9) as well as in the bottom strands (10-14 and 15-19), this symmetry is not reflected in the optimized topology. Instead, a symmetry of left and right is observed, resulting from the control and stream device positions. This symmetry might look odd to the engineer even if being optimal. As a relieve symmetry constraints as given in [34] can be used. All signals were routed correctly and all signal power levels are within the acceptable range of their respective receivers. A careful inspection of the optimization result uncovers a shortcoming in our cost function: While two signals to the Seat Unit with number 11 follow short paths from start to destination, one signal is not optimal in terms of hop count. Instead of using the available core of the connection 10-11, it runs via Switch 14. However, since the alternative path with fewer hops does not result in a better objective function value, it is not picked by the optimizer.

VI. Conclusion

The demonstration with the small IFE system shows that the method is appropriate for the desired topology design. It became clear in that further routing constraints (e.g. hop count and segregation) may be needed to limit the signals routed through a device. The used domain-specific model OAAM

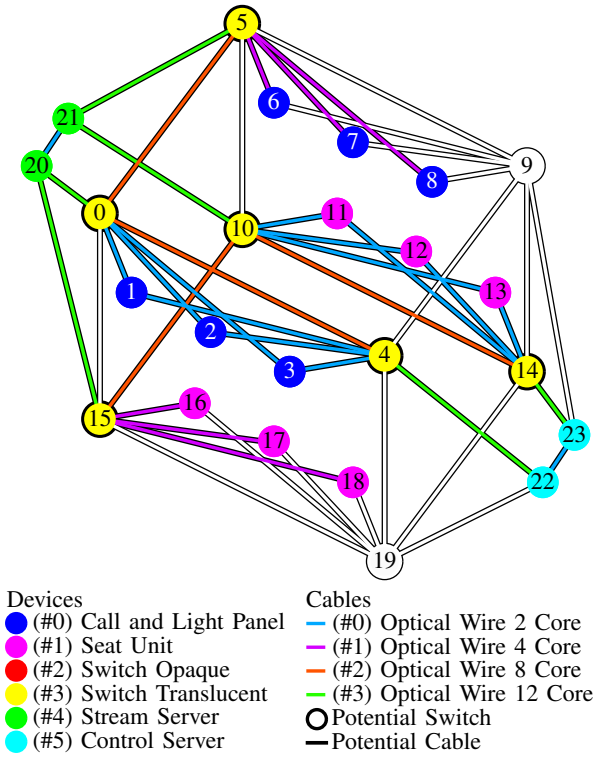

Fig. 4. Spatial representation of the installation space and the optimal solution of IFE scenario.

includes ways to specify such constraints, which were not considered so far. The problem size is critical since Big-M constraints can quickly lead to infeasible calculation times. For the IFE scenario it contains 18000 variables and 50000 constraints. Surprisingly, the demonstration model is solved in 23 min. Optimization times in the order of several hours to days can be expected for a real aircraft. An alternative can be an MILP model, which selects from pre-calculated paths instead of building the path. The fact that only one single signal is transmitted in one core is a limitation in practice. Future investigations should, therefore, look at relaxing this limitation. It makes sense include other optical transmission techniques, e.g. Wavelength-Division-Multiplexing (WDM). In conclusion, it can be stated that topology optimization of optical networks is feasible within an acceptable time and provides added value to the design of aircraft systems.

References

[1] B. Annighöfer, "Model-based architecting and optimization of distributed integrated modular avionics," Dissertation, Hamburg University of Technology, Hamburg, 2015.

[2] J.-B. Itier, "IMA1G - Genesis and Results," SCARLETT MOSCOW - 1st Forum, September 2009.

[3] J. Lopez and J.-B. Itier, "Afdx network with a passive optical network," Patent US 9 148 222 (B2), 2015.

[4] A. Al Sheikh, O. Brun, M. Chéramy, and P.-E. Hladik, "Optimal design of virtual links in afdx networks," *Real-Time Systems*, pp. 1–29, 2012. [Online]. Available: http://dx.doi.org/10.1007/s11241-012-9171-z

[5] D. Carta, J. de Oliveira, and R. Starr, "Allocation of avionics communication using boolean satisfiability," in *DASC*, 2012

[6] J. Falk, F. Dürr, and K. Rothermel, "Exploring Practical Limitations of Joint Routing and Scheduling for TSN with ILP," in *RTCSA*, 2018

[7] F. Smirnov, M. Glaß, F. Reimann, and J. Teich, "Optimizing message routing and scheduling in automotive mixed-criticality time-triggered networks," in *DAC*, 2017.

[8] S. Singh, "Routing algorithms for time sensitive networks," Stuttgart, 2017.

[9] A. Ebrahimzadeh, A. G. Rahbar, and B. Alizadeh, "Binary quadratic programming formulation for routing and wavelength assignment problem in all-optical wdm networks," *Optical Switching and Networking*, vol. 10, no. 4, pp. 354–365, 11 2013.

[10] K. Kumari, S. J. Nanda, and R. K. Maddila, "Optimal path determination in a survivable virtual topology of an optical network using ant colony optimization," in *Proceedings of Sixth International Conference on Soft Computing for Problem Solving*, 2017, pp. 48–58.

[11] O. Ayoub, A. Bovio, F. Musumeci, and M. Tornatore, "Survivable virtual network mapping in filterless optical networks," in *ONDM*, 2020.

[12] F. Dürr and N. G. Nayak, "No-wait Packet Scheduling for IEEE Time-sensitive Networks (TSN)," in *RTNS*, 2016

[13] D. Ergenc, J. Rak, and M. Fischer, "Service-based resilience via shared protection in mission-critical embedded networks," *IEEE Transactions on Network and Service Management*, pp. 1–1, 2021.

[14] L. M. M. Zorello, S. Troia, M. Quagliotti, and G. Maier, "Power-aware optimization of baseband-function placement in cloud radio access networks," in *ONDM*, 2020.

[15] O. Acevedo, D. Kagaris, K. Poluri, H. Ramaprasad, and S. Warner, "Towards optimal design of avionics networking infrastructures," in *DASC*, 2012

[16] A. Lübke and H.-C. Reuss, "Optimierung der bordnetzarchitektur mit hilfe genetischer algorithmen," *ATZ - Automobiltechnische Zeitschrift*, vol. 102, no. 6, pp. 436–442, 2000.

[17] Z. Li, H. Xia, Y. Zhang, J. Qi, S. Wu, and S. Gu, "Multi-objective network optimization combining topology and routing algorithms in multi-layered satellite networks," *Science China Information Sciences*, vol. 61, no. 8, 2018.

[18] A. K. Gupta and W. J. Dally, "Topology optimization of interconnection networks," *IEEE Computer Architecture Letters*, vol. 5, no. 1, 2006.

[19] A. Z. Kasem and J. Doucette, "Incremental optical network topology optimization using meta-mesh span restoration," in *DRCN*, 2011.

[20] I. J. Rahman, A. R. Zain, and N. R. Syambas, "A new heuristic method for optical network topology optimization," in *ICWT*, 2016.

[21] I. Filippini and M. Cesana, "Topology optimization for hybrid optical/wireless access networks," *Ad Hoc Networks*, vol. 8, no. 6, 2010.

[22] A. Agata and K. Nishimura, "Suboptimal PON network designing algorithm for minimizing deployment cost of optical fiber cables," in *ONDM*, 2012.

[23] A. de Sousa, A. Tomaszewski, and M. Pioro, "Bin-packing based optimisation of EON networks with s-BVTs," in *ONDM*, 2016.

[24] M. Youssef, S. A. Zahr, and M. Gagnaire, "Cross optimization for RWA and regenerator placement in translucent WDM networks," in *ONDM*, 2010.

[25] A. Kokangul and A. Ari, "Optimization of passive optical network planning," *Applied Mathematical Modelling*, vol. 35, no. 7, 2011.

[26] B. Annighöfer, C. Reif, and F. Thieleck, "Network topology optimization for distributed integrated modular avionics," in *DASC*, 2014.

[27] B. Annighoefer and A. Zeyher, "Multi-core fiber and power-limited optical network topology optimization with MILP.",2021. https://arxiv.org/abs/2103.16981

[28] "The foa reference for fiber optics - optical fiber," The Fiber Optic Association, Inc., 1999-2018.

[29] "Calculating fiber optic loss budgets," The Fiber Optic Association, Inc., 2004-2018.

[30] P. Belotti, P. Bonami, M. Fischetti, A. Lodi, M. Monaci, A. Nogales-Gómez, and D. Salvagnin, "On handling indicator constraints in mixed integer programming," *Computational Optimization and Applications*, vol. 65, 2016.

[31] G. G. Brown and R. Dell, "Formulating integer linear programs: A rogues' gallery," *Informs Transactions on Education*, vol. 7, 01 2007.

[32] B. Annighoefer, "An open source domain-specific avionics system architecture model for the design phase and self-organizing avionics," in *SAE AeroTech Americas*, 2019.

[33] *HITRONIC® TORSION*, U.I. Lapp GmbH, 9 2014.

[34] B. Annighoefer, C. Nil, J. Sebald, and F. Thielecke, "Structured and symmetric IMA architecture optimization: Use case Ariane launcher," in *DASC*, 2015.